

Persistence of hierarchical network organization and emergent topologies in models of functional connectivity

Ali Safari^a, Paolo Moretti^{a,*}, Ibai Diez^{b,c}, Jesus M. Cortes^{d,e,f}, Miguel Ángel Muñoz^{g,h}

^a*Institute of Materials Simulation, Friedrich-Alexander-Universität Erlangen-Nürnberg, Dr.-Mack-Str. 77, D-90762 Fröh, Germany*

^b*Functional Neurology Research Group, Department of Neurology, Massachusetts General Hospital, Harvard Medical School, Boston, MA 02115, USA*

^c*Gordon Center, Department of Nuclear Medicine, Massachusetts General Hospital, Harvard Medical School, Boston, MA 02115, USA*

^d*Biocruces-Bizkaia Health Research Institute, Barakaldo, Spain*

^e*Department of Cell Biology and Histology. University of the Basque Country (UPV/EHU), Leioa, Spain*

^f*IKERBASQUE: The Basque Foundation for Science, Bilbao, Spain*

^g*Departamento de Electromagnetismo y Física de la Materia, Universidad de Granada, Granada E-18071, Spain*

^h*Instituto Carlos I de Física Teórica y Computacional, Universidad de Granada, Granada E-18071, Spain*

Abstract

Functional networks provide a topological description of activity patterns in the brain, as they stem from the propagation of activity on the anatomical, or structural network of synaptic connections, which possess a hierarchical organization. While it is assumed that structural networks shape their functional counterparts, it is also hypothesized that alterations of brain activity may come with transformations of functional connectivity, and possibly its deviation from the hierarchical topology. In this computational study, we introduce a novel methodology to monitor the persistence and breakdown of hierarchical order in functional networks, generated from simulations of activity spreading on both synthetic and real structural connectomes. We show that hierarchical connectivity is persistent in the quasi-critical regime associated with optimal processing capabilities and normal brain function (Griffiths phase) and breaks down in

*Corresponding author

Email address: paolo.moretti@fau.de (Paolo Moretti)

states deviating from this regime, often associated with pathological conditions. Our results offer important clues for the study of optimal neurocomputing architectures and processes, which are capable of tuning patterns of activity and information flow, and show how the hierarchical topology and its quasi-critical functional counterpart provide an effective balance between local specialized processing and global integration.

Keywords:

brain networks, functional connectivity, hierarchical modular networks

1. Introduction

Recent convergence of neuroscience and network science opens up new opportunities to approach the study of brain function [1, 2, 3]. A fundamental issue in this context is how *structure* and *function* are related [4, 5, 6, 7, 8]. In the context of network neuroscience, structure refers to the network mappings of the brain, also known as connectomes, as derived from the actual anatomical connections between brain regions [9, 10]. Structural connectivity (SC) is thus encoded in networks where nodes are coarse-grained representations of specific brain regions, and the links express the presence of white-matter based connections between pairs of nodes, while weights associated with links conventionally measure the number of such connections. Structural networks are then represented by undirected, weighted, non-negative and sparse adjacency matrices, effectively containing the anatomical routing information of a brain. Functional connectivity (FC), instead, arises from neural activity correlations rather than actual anatomical pathways. As activity correlations can be measured between any pair of nodes, the matrix representations for functional networks differ substantially from those for structural networks in that they lose the sparse property. FC matrices are dense and equivalent sparse network representations can only be obtained by applying arbitrary thresholds. As a further source of complication, FC matrices lose the non-negativity of SC matrices too, as activity correlations are signed, pointing to both correlations and anti-correlations. This

aspect makes the application of thresholds even more complex, not to mention subject to arbitrariness, as in choosing for instance to exclude anti-correlations, or to study correlations and anti-correlations separately.

We note that in spite of this complexity, FC data have been recorded for years now and has led to groundbreaking advances in the the understanding of brain function, both at the clinical level [11, 12, 13, 14], where FC data has been successfully related to the occurrence of brain pathologies, and the graph theoretical level, where FC data allowed the introduction of statistical physics concepts such as scale invariance, avalanches, criticality and localization in the brain [15, 16, 17, 18, 19, 20]. Advances in acquisition and analysis of FC data have allowed the introduction of novel and challenging concepts, such as that of dynamical FC, the ambitious study of time fluctuation and evolution of functional networks, obtained through the recording of multiple functional networks, each one over a short time window [21, 22]. The question remains, however, what topological information is lost when thresholds are applied.

Structural brain networks [23, 24] are well known examples of biological systems, which exhibit a hierarchical modular structure. Hierarchical modular organization is often described by simple mathematical models of synthetic hierarchical modular networks (HMNs). Can we say the same about functional networks? How definitive can the answer to this question be, if functional network topology can vary so wildly because of arbitrary threshold choices? How persistent the hierarchical organization of structural network is in FC data, upon applying different threshold and, more importantly, in different states of neural activity? Are deviations between SC and FC data representative of pathological states?

Assessing the similarity between structural and functional connectivity represents a crucial aspect of the current structure-function debate. Similarity measures were proposed in the past (see for instance [8]), highlighting how similarity itself may be non-trivially dependent on the choice of thresholds used to extract functional networks. In this work we follow a more fundamental approach, in the attempt to formulate a criterion to decide if a functional network

is hierarchical and to do so irrespective of threshold choices.

The interest in the hierarchical organization of brain activity patterns is rooted in the observation that hierarchical (and hierarchical modular) networks exhibit desirable properties of robustness. Remarkably, hierarchical networks do not exhibit a single percolation threshold: upon varying the control parameter p (i.e. upon removing a fraction $1 - p$ of links or nodes) power-law distributions of connected component sizes are encountered for all values of p [25, 16]. The functional counterparts to this simple structural property are striking i) activity in hierarchical models of the brain is sustained even without fine-tuning of inhibition mechanisms [26]; ii) avalanches of neural activity are power law distributed in size without the need to fine tune spreading control parameters [16, 17], rationalizing the experimental observation of scale invariant activity patterns [27]; iii) simple dynamic models, normally displaying clear-cut tipping points (phase transitions), exhibit instead extended quasi-critical parameter intervals (e.g. Griffiths phases [28, 29, 30, 17, 31, 18, 19]), where activity propagates by rare region effects and states of local coherence emerge as chimera states [32]. These observations corroborate the view that the hierarchical organization of the brain is responsible for its ability to localize activity, avoiding the opposing tendencies where active states die out (as encountered in advance stages in neurodegenerative diseases) or invade the systems (typical of epileptic seizures). From the perspective of neurocomputing and information processing, HMNs thus provide an optimal architecture, which ensures the balance of activity segregation and integration [33], and results in enhanced computational capabilities, large network stability, maximal variety of memory repertoires and maximal dynamic range [17].

In the optimal quasi-critical phase described above, the hierarchical SC network structure promotes the formation of activity patterns that we associate with normal brain function. But is the resulting FC network hierarchical too? To answer this question, we identify *hierarchical functional networks* based on their spectral properties. In particular, we focus on the well known property of vanishing spectral gaps, which we use as a measure of the hierarchical organiza-

tion [17]. While the spectral characterization of HMNs is much more complex, vanishing spectral gaps have been directly related with the desirable features of sustained activity and local coherence, which make hierarchical networks unique and, more importantly, constitute the reason why hierarchical organization is essential in brain networks. In the following, we generate FC data from Monte Carlo simulations of simple models of activity spreading in synthetic HMN models and on real SC data and show that, independently of the choice of thresholds, functional networks generated in the quasi-critical regime always display hierarchical organization, a feature that is lost as soon as FC data is produced in the super-critical regime – i.e. *above* quasi-critical regime. Our results offer important insights regarding the topological changes that FC data undergoes in pathological states (the super-critical regime), providing clues for FC analysis as a diagnostic tool. At the same time, our methodology provides a new tool for the analysis of persistent features in functional data, whose appearance is not an artifact of an arbitrary threshold choice.

2. Materials and methods

Structural networks. We use computer generated models of HMNs, in order to mimic realistic structural networks. As different types of algorithms are used in the literature to generate HMNs [26, 34, 17, 19, 20], in the following we refer the model proposed in [20] without loss of generality. We call α the *connectivity strength* of a HMN, as it is the main parameter controlling the emerging topology. The network is organized in densely connected modules of size M_0 , which represent the level 0 of a hierarchy of links. At each hierarchical level $i > 0$, super-modules of size $M_i = 2^i M_0$ are formed, joining sub-modules of size M_{i-1} by wiring their respective nodes with probability $\pi_i = \alpha/4^i$: the average number of links between two modules at level i will thus be $n_i = \pi_i M_{i-1}^2 = \alpha(M_0/2)^2$, i.e. proportional to α , regardless of the value of i . For a generic dynamic process running on a HMN in the $N \rightarrow \infty$ limit, the effect of lowest-level modules becomes negligible (relegated to transient time scales) and the time asymptotics

are dominated by the hierarchical organization: in this regime α becomes the only relevant construction parameter. We remark that, being n_i the number of links between any two modules of size M_{i-1} , the maximum value of n_i is given by M_0^2 , so that α can take values in the interval $4/M_0^2 \leq \alpha \leq 4$.

Graph spectra. We identify an unweighted graph through its adjacency matrix A_{ij} , whose generic element ij is 1 if nodes i and j are connected, and 0 otherwise. This choice represent a simplification of the more complex case of a weighted graph, where each link between i and j comes with a weight W_{ij} . The spectrum of the unweighted graph is given by the eigenvalues of A_{ij} . The Perron-Frobenius theorem ensures that the eigenvalue of largest modulus λ_1 is real and positive. The spectral gap g is then defined as the difference in modulus between λ_1 and the second eigenvalue λ_2 . Here we deal with undirected HMNs, so that A_{ij} is symmetric, and $g = \lambda_1 - \lambda_2$. We can also compute the Laplacian spectrum of a graph, which consists of the eigenvalues of the graph Laplacian $L_{ij} = \delta_{ij} \sum_l k_j - A_{ij}$, which provides a discretization of the Laplace-Beltrami operator. Here $k_i = \sum_j A_{ij}$ is the degree of node i . If A_{ij} is symmetric, L_{ij} is symmetric and positive semi-definite, and the spectral gap g_L is defined as the modulus of its smallest nonzero eigenvalue. An alternative discretization of the Laplace-Beltrami operator is provided by the normalized Laplacian matrix $\mathcal{L}_{ij} = \delta_{ij} - A_{ij}/\sqrt{k_i k_j}$, for which we can define the spectral gap $g_{\mathcal{L}}$ as we did for L . For completeness, we mention the random walk laplacian, which enters the master equation of the random walk, and which has the same spectrum of eigenvalues as \mathcal{L} [35].

Dynamic model. We simulate dynamics in HMN models of the brain using a null model of activity propagation in network, namely SIS dynamics. Nodes can be either active (infected I) or inactive (susceptible S); in terms of neural dynamics an active node corresponds to an active region in the brain, which can activate an inactive neighboring region with a given probability κ , and which can be deactivated at rate μ (which we set to 1 without loss of generality) due to exhaustion of synaptic resources. In the general case, SIS dynamics result

in a critical value $\kappa = \kappa_c$, above which activity invades the system indefinitely (super-critical regime, in the following). In the case of HMNs, values of $\kappa < \kappa_c$ (quasi-critical regime) constitute a Griffiths phase and are associated with rare region effects and slow activity relaxation, pointing to an effective model for normal brain function. The use of such simple dynamical models has proven effective as a probing tool to understand paramount features of brain activity [26, 17].

Functional data. We analyze FC data by storing co-activation matrices [36, 37]. We fix a time interval I for every set of simulations and value of κ , and we generate a matrix C_{ij} with generic ij element equal to the probability that nodes i and j are simultaneously active. We average C_{ij} across multiple realizations of the dynamics. We consider a threshold θ and generate the adjacency matrix of the functional network for each θ by unitization, i.e. $A_{ij}(\theta) = H(\theta - C_{ij})$, where $H(\cdot)$ denotes the Heaviside step function. When recording functional data, we focus on a single realization of the structural network hosting the dynamics, mimicking a realistic scenario in which diagnostics are conducted on a single subject.

Mapping to percolation problem. For every functional network of adjacency matrix $A_{ij}(\theta)$, we vary θ continuously and we monitor how the network evolves by measuring two *order parameters*: i) the size of the largest connected component s_1 ; ii) the spectral gap g (and its Laplacian variants for completeness). For $\theta \approx 0$ the network is fully connected, $s_1 = N$ and $g = N$ ($g_L = N$, $g_{\mathcal{L}} = 1$). For $\theta \approx 1$ the network is fragmented, $s_1 = 1$ and $g \approx 0$ (as its Laplacian counterparts). For intermediate θ the network undergoes a percolation-like phase transition, however s_1 and g may behave differently. In this work, we precisely focus on the different behavior s_1 and g , showing how hierarchical functional networks are those characterized by two separate transitions.

3. Results

Our aim here is to find an effective way to assess if a functional network is hierarchical, thus mimicking the topology of the underlying structural network, or if activity correlations result in a different, emergent topology. To this end, we define the concept of hierarchical functional network as follows. Since many of the desirable dynamic properties of hierarchical modular networks (rare region effects, generic criticality, localization) can be traced back to their small spectral gaps g (as well as g_L and $g_{\mathcal{L}}$), we define a hierarchical functional network as a network that i) is generated by activity patterns on a structural HMN; ii) in a finite range of θ , possesses vanishing spectral gaps, while still being connected (i.e. not fragmented). Requirement ii) ensures that the vanishing spectral gap property is not a trivial consequence of a network breaking into many connected components.

Any functional network undergoes two phase transitions as the threshold θ is increased, where s_1 and g act as order parameters. According to the criterion we introduced above, in a hierarchical functional network these two transitions are well separated and there exist a threshold interval in which the spectral gap g decreases by orders of magnitude (the order of N), while s_1 remains maximum (the network remains connected). By running our simulations on synthetic HMNs and acquiring functional data as described in the Materials and methods section, we can see that this definition of hierarchical functional networks describes exactly what happens in the quasi-critical regime, which we associate with normal brain function, as shown in Figure 1. Simulation data for the quasi-critical case show that upon increasing the threshold θ the network undergoes a trivial percolation-like transition (red dotted line), as the largest connected component size s_1 (red circles) changes from the network size N (when the network is connected) to 1 (when the network is fragmented). The spectral gap g (blue squares) too exhibits an expected phase transition (blue dashed line), from N (when the functional network is dense and fully connected) to vanishing values. These two transitions however do not coincide and a range

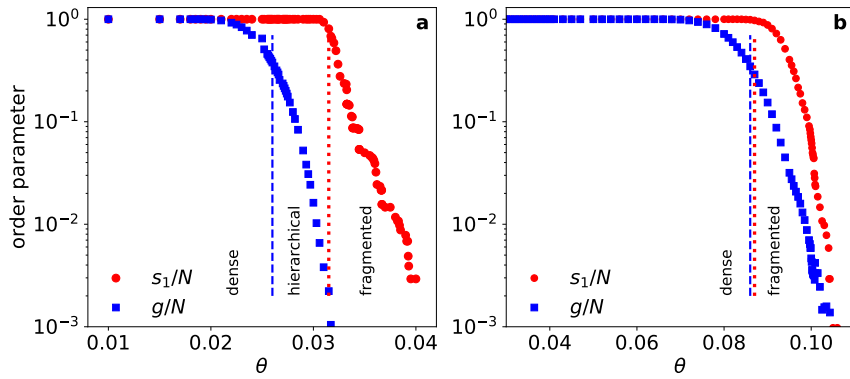


Figure 1: Persistence and breakdown of hierarchical organization. a) Largest connected component size s_1 and spectral gap g in the quasi-critical regime ($\kappa \leq \kappa_c$), or Griffiths phase, for co-activation matrices $A_{ij}(\theta)$, generated by activity propagation dynamics on a single structural HMN. A range of threshold values θ exists, where the resulting functional network is connected ($s_1 = N$) and has vanishing spectral gaps (by up to three orders of magnitude, the theoretical limit given by the system size). We observed no significant variations changing HMN realization. b) Same as a), in the super-critical regime ($\kappa > \kappa_c$). No significant drop in spectral gap is recorded while the network is intact, pointing to the loss of hierarchical order. For as long as the network is connected ($s_1 = N$), g drops by negligible amounts, and remains of the order of N .

of control parameter values θ emerges, where the network is connected ($s_1 = N$), but spectral gaps vanish ($g \rightarrow 0$), decreasing by up to three orders of magnitudes. This finite range of values of θ ensures that when the functional network is not trivial (i.e. not fully connected and not fragmented), it is hierarchical.

The strength of this result resides in its dependence on the dynamical regime that we simulate. We just showed that the functional network is hierarchical in the quasi-critical regime, more precisely in the Griffiths phase. But, what happens in the super-critical regime, obtained for activation rates $\kappa > \kappa_c$, which normally is associated with abnormal (excessive) neural activity? Figure 1b shows that in this regime the two phase transitions almost coincide and, more importantly, there is no range of θ , where the functional network is connected and the spectral gaps vanish. The functional network is not hierarchical, since whenever it is connected it has large spectral gaps (which only decrease slightly, still maintaining huge values, and not dropping by an amount comparable to N), and its topology is fully an emergent property of the dynamics.

In our study, we consider structural HMNs of size $N = 1024$, which already result on dense co-activation matrices of 1048576 elements, thus making the rest of the study computationally intensive. At the same time, we note that most experimentally acquired connectomes belong in the same size range, allowing for a direct comparison as we will show later on in this paper.

The picture of hierarchical functional networks that develop an emergent, non-hierarchical topology in the super-critical regime is further corroborated by the study of the degree distributions of such networks, as shown in Figure 2. In the quasi-critical phase, and for values of θ within the range highlighted in Figure 1a, degree distributions have power-law tails with continuously varying exponents. This form of *generic* scale invariance has the same structural origin as the one observed in avalanche size measurements in this same regime [17]: the hierarchical organization induces rare region effects, which are reflected both in avalanches and in the topology of the functional network. In the super-critical regime instead, degree distributions display heavier power-law tails with an emergent, limiting exponent close to $3/2$.

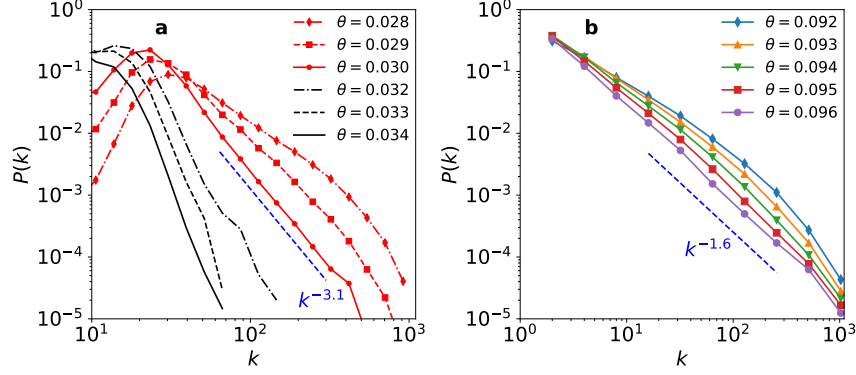


Figure 2: Degree distributions of functional networks. a) Quasi-critical regime. Red curves are obtained for values of θ producing networks with maximum separation between s_1 and g . Larger values of θ (black curves) occur when the network is close to failure ($s_1 \rightarrow 0$). In order to improve the statistical sampling, multiple functional networks (60) are generated from the same HMN and their degree distributions averaged. A data set showing the case of $P(k) k^{-3.1}$ as an estimate for the limiting distribution is added. b) Super-critical regime. Degree distribution change dramatically, displaying much heavier tails.

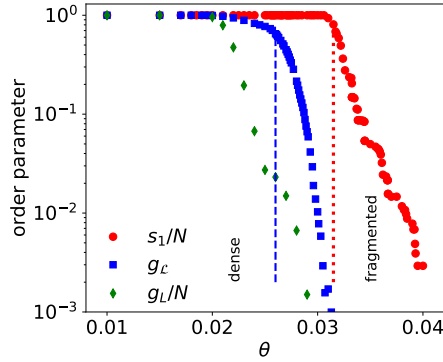


Figure 3: Persistence of hierarchical organization, as from the study of laplacian matrices. Data is obtained as in Figure 1a, employing spectral gaps from the graph laplacian L and the normalized laplacian \mathcal{L} . Data for s_1 is the same as in Figure 1a and is reported here for comparison.

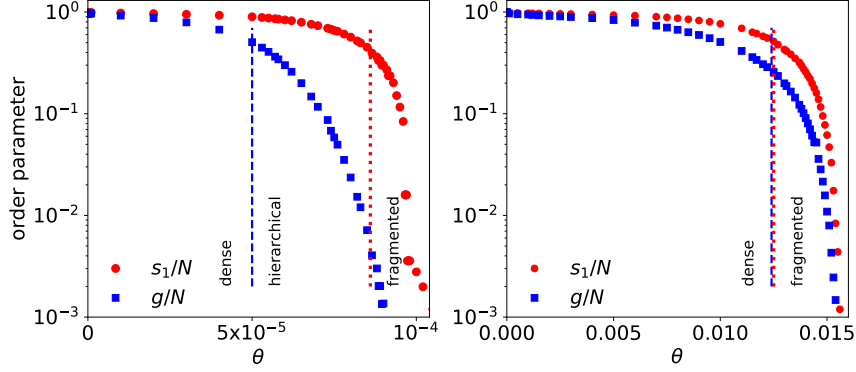


Figure 4: Persistence and breakdown of hierarchical organization of functional networks generated from a single real connectome. Quasi-critical regime (a) and super-critical regime (b). Results are as for the synthetic HMN case shown in Figure 1

Our main result of hierarchical functional network organization in the quasi-critical regime has been obtained above using the definition of spectral gap g applied to the adjacency matrix $A_{ij}(\theta)$. This choice is motivated by the fact that $A_{ij}(\theta)$ is produced by an SIS process, which is linearized by the adjacency matrix A_{ij} of the underlying structural network. Nevertheless, one may wonder if the result above extends to laplacian matrices [35], which are of interest in problems of transmission, diffusion and, more importantly in the case of brain dynamics, synchronization. Figure 3 shows that our main result carries over to the case of laplacian matrices, both in the non-normalized variant L (historically, the Kirchhoff laplacian) and in the normalized one \mathcal{L} (isospectral to the random walk laplacian).

Given the relevance of our results in the field of computational neuroscience, and in order to prove that they are not artifacts of our specific HMN construction method, we performed the same numerical study by running our simulations on real human connectomes of sizes comparable to the ones considered above ($N = 2514$). Our results, shown in Figure 4 are striking as they show how the exact same fingerprints of hierarchical functional organization in the quasi-critical case emerge by simulating activity propagation simulations on SC networks. Data

shown here is produced from the structural network of a single healthy subject. While we performed the tests on SC data from multiple subjects, we noticed that subject variability amounts to quantitative changes, while the same qualitative behavior is found, irrespective of the subject (not shown in Figure 4).

More in detail, data available to us are from 30 healthy subjects (14 males, 16 females) with age between 22 and 35 were used in this study. Data were provided by the Human Connectome Project, WU-Minn Consortium (Principal Investigators: David Van Essen and Kamil Ugurbil; 1U54MH091657) funded by the 16 NIH Institutes and Centers that support the NIH Blueprint for Neuroscience Research; and by the McDonnell Center for Systems Neuroscience at Washington University. To build the connectivity matrices (for further details see [38]), we processed the same-subject structure-function triple acquisitions of magnetic resonance imaging (MRI) – see Appendix for details on acquisition parameters – consisting of: 1. High-resolution anatomical MRI (used for the mask segmentation of gray matter, white matter and cerebrospinal fluid, and for the transformation to common-space of the functional and the diffusion data), 2. Functional MRI at rest (used for extracting region time series of the blood-oxygen-dependent signal, after removal of movement artifacts and physiological noise, but not the global signal regression), and 3. Diffusion MRI (used for building SC matrices after fitting a diffusion tensor to each voxel, running a deterministic tractography algorithm using the UCL Camino Diffusion MRI Toolkit [39], and counting the number of streamlines connecting all pairs within the $N = 2514$ regions, each one containing on average 66 voxels).

4. Conclusion and discussion

The relationship between structure and function in brain networks remains to this day a field of enormous interest. The ultimate goal of devising diagnostic tools that leverage concepts of network theory applied to SC connectivity data begs for a deeper understanding of how dynamic patterns originate from structural motifs, or to which extent they self-organize irrespective of those motifs.

What we introduced here is a minimal model, which however captures some essential aspects of this complex balance. In the quasi-critical regime, activity patterns are strongly localized and result in a FC network which closely mimics the SC hierarchical patterns, although in a dynamic way, inheriting its basic spectral property. This is not to say that activity correlations do not play a role: the FC degree distributions do not replicate those of SC, they in fact are power laws with continuously varying exponents, in analogy with avalanche size distributions stemming from rare region effects.

In the super-critical regime, which represents a pathological state akin to epilepsy, the spectral fingerprint of hierarchical networks is lost and functional connectivity earns a global and much denser network topology. While it was shown in the past that networks with localized structures host localized activity patterns also in the super-critical phase [40], something we were able to confirm in HMN models of brain activity [20], the change in spectral properties and degree distributions points to a significant reorganization of dynamics and correlations, in which modules mutually reactivate (or mutually reinfect, as in similar models of epidemics [41, 42].).

Our methodology addresses the analysis of activity correlation data without fixing an arbitrary threshold. Thresholds are treated as a control parameter in a phase diagram, which is analyzed in its entirety. We note that the mapping of this phase diagram to that of a percolation problem is not new [33, 43]. Here we used a similar methodology to show how, in the quasi-critical regime, threshold values which correspond to non-trivial functional network topologies (fully connected, fragmented) also lead to the non trivial property of small spectral gaps, which allows us to conclude that the functional networks effectively inherit the hierarchical organization of the structural ones.

We believe that our work serves as a proof-of-concept study, for more complex applications in which multiple spectral indicators are considered, and in which FC is inferred from real time series, rather than from numerical simulations. The simple methodology we adopt here, based on co-activations, has clear advantages while generating functional networks under minimal assump-

tions, thus avoiding normalization practices which might introduce variability in the results. At the same time, our study can also be conducted on FC data extracted as Pearson correlation, allowing for instance the separation of correlation and anti-correlation effects.

Our work of course relies on essential simplifications of the original neuroscience problem. Namely our simulated dynamics is a simplification of neural activation processes. Nevertheless, we believe that our results provide useful insights regarding the extent to which structure and function are connected in brain networks, and how pathological states can be accompanied by radical shifts in functional connectivity. We believe that our spectral analysis of persistent and emergent topologies in FC data sheds light on the relationship between optimal architectures and tuneable performance in the broader context of neurocomputing.

References

- [1] O. Sporns, D. R. Chialvo, M. Kaiser, C. C. Hilgetag, Organization, development and function of complex brain networks, *Trends in cognitive sciences* 8 (2004) 418–425.
- [2] E. Bullmore, A. Barnes, D. S. Bassett, A. Fornito, M. Kitzbichler, D. Meunier, J. Suckling, Generic aspects of complexity in brain imaging data and other biological systems, *Neuroimage* 47 (2009) 1125–1134.
- [3] O. Sporns, *Networks of the brain*, MIT Press.
- [4] C. Zhou, L. Zemanová, G. Zamora, C. C. Hilgetag, J. Kurths, Hierarchical organization unveiled by functional connectivity in complex brain networks, *Phys. Rev. Lett.* 97 (2006) 238103. doi:10.1103/PhysRevLett.97.238103.
- [5] M. Müller-Linow, C. C. Hilgetag, M. T. Hütt, Organization of excitable dynamics in hierarchical biological networks, *PLoS Comput. Biol.* 4 (2008) e1000190.

- [6] E. Bullmore, O. Sporns, The economy of brain network organization, *Nature Rev. Neurosci.* 13 (2012) 336–349.
- [7] O. Sporns, Structure and function of complex brain networks, *Dialogues Clin. Neurosci.* 15(3) (2013) 247–62.
- [8] I. Diez, P. Bonifazi, I. Escudero, B. Mateos, M. A. Muñoz, S. Stramaglia, J. M. Cortes, A novel brain partition highlights the modular skeleton shared by structure and function, *Scientific reports* 5 (2015) 10532.
- [9] R. Craddock, S. Jbabdi, C. Yan, J. Vogelstein, F. Castellanos, A. D. Martino, C. Kelly, K. Heberlein, S. Colcombe, M. Milham, Imaging human connectomes at the macroscale, *Nat Methods* 10 (2013) 524–539. doi:10.1038/nmeth.2482.
- [10] A. Fornito, A. Zalesky, E. Bullmore, *Fundamentals of Brain Network Analysis*, Academic Press, 2016.
- [11] B. B. Biswal, M. Mennes, X.-N. Zuo, S. Gohel, C. Kelly, S. M. Smith, C. F. Beckmann, J. S. Adelstein, R. L. Buckner, S. Colcombe, A.-M. Dugonowski, M. Ernst, D. Fair, M. Hampson, M. J. Hoptman, J. S. Hyde, V. J. Kiviniemi, R. Kötter, S.-J. Li, C.-P. Lin, M. J. Lowe, C. Mackay, D. J. Madden, K. H. Madsen, D. S. Margulies, H. S. Mayberg, K. McMahon, C. S. Monk, S. H. Mostofsky, B. J. Nagel, J. J. Pekar, S. J. Peltier, S. E. Petersen, V. Riedl, S. A. R. B. Rombouts, B. Rypma, B. L. Schlaggar, S. Schmidt, R. D. Seidler, G. J. Siegle, C. Sorg, G.-J. Teng, J. Veijola, A. Villringer, M. Walter, L. Wang, X.-C. Weng, S. Whitfield-Gabrieli, P. Williamson, C. Windischberger, Y.-F. Zang, H.-Y. Zhang, F. X. Castellanos, M. P. Milham, Toward discovery science of human brain function, *Proceedings of the National Academy of Sciences* 107 (10) (2010) 4734–4739. doi:10.1073/pnas.0911855107.
- [12] M. Fox, M. Greicius, Clinical applications of resting state functional connectivity, *Frontiers in Systems Neuroscience* 4 (2010) 19. doi:10.3389/fnsys.2010.00019.

- [13] D. V. Essen, K. Ugurbil, E. Auerbach, D. Barch, T. Behrens, R. Bucholz, A. Chang, L. Chen, M. Corbetta, S. Curtiss, S. D. Penna, D. Feinberg, M. Glasser, N. Harel, A. Heath, L. Larson-Prior, D. Marcus, G. Michalar-eas, S. Moeller, R. Oostenveld, S. Petersen, F. Prior, B. Schlaggar, S. Smith, A. Snyder, J. Xu, E. Yacoub, The human connectome project: A data ac-
quisition perspective, *NeuroImage* 62 (4) (2012) 2222 – 2231. doi:<https://doi.org/10.1016/j.neuroimage.2012.02.018>.
- [14] M. Lee, C. Smyser, J. Shimony, Resting-state fmri: A review of methods
and clinical applications 34 (10) (2013) 1866–1872. doi:[10.3174/ajnr.A3263](https://doi.org/10.3174/ajnr.A3263).
- [15] A. Haimovici, E. Tagliazucchi, P. Balenzuela, D. R. Chialvo, Brain organi-
zation into resting state networks emerges at criticality on a model of the
human connectome, *Physical Review Letters* 110 (2013) 178101.
- [16] E. J. Friedman, A. S. Landsberg, Hierarchical networks, power laws, and
neuronal avalanches, *Chaos* 23 (2013) 013135.
- [17] P. Moretti, M. A. Muñoz, Griffiths phases and the stretching of criticality
in brain networks, *Nature Commun.* 4 (2013) 2521.
- [18] G. Ódor, Localization transition, lifschitz tails, and rare-region effects in
network models, *Phys. Rev. E* 90 (2014) 032110.
- [19] G. Ódor, R. Dickman, G. Ódor, Griffiths phases and localization in hierar-
chical modular networks, *Sci. Rep.* 5 (2015) 14451.
- [20] A. Safari, P. Moretti, M. A. Muñoz, Topological dimension tunes activity
patterns in hierarchical modular networks, *New Journal of Physics* 19 (11)
(2017) 113011. doi:[10.1088/1367-2630/aa823e](https://doi.org/10.1088/1367-2630/aa823e).
URL <https://doi.org/10.1088/1367-2630/aa823e>
- [21] J. Cabral, M. L. Kringelbach, G. Deco, Functional connectivity dy-
namically evolves on multiple time-scales over a static structural

- connectome: Models and mechanisms, *NeuroImage* 160 (2017) 84–96.
doi:10.1016/j.neuroimage.2017.03.045.
URL <https://linkinghub.elsevier.com/retrieve/pii/S1053811917302537>
- [22] M. G. Preti, T. A. Bolton, D. Van De Ville, The dynamic functional connectome: State-of-the-art and perspectives, *NeuroImage* 160 (2017) 41–54. doi:10.1016/j.neuroimage.2016.12.061.
URL <https://linkinghub.elsevier.com/retrieve/pii/S1053811916307881>
- [23] O. Sporns, G. Tononi, R. Kötter, The human connectome: A structural description of the human brain, *PLoS Comput. Biol.* 1(4) (2005) e42.
- [24] P. Hagmann, L. Cammoun, X. Gigandet, R. Meuli, C. J. Honey, V. J. Wedeen, O. Sporns, Mapping the structural core of human cerebral cortex, *PLoS Biol.* 6 (2008) e159.
- [25] S. Boettcher, J. L. Cook, R. M. Ziff, Patchy percolation on a hierarchical network with small-world bonds, *Phys. Rev. E* 80 (2009) 041115.
- [26] M. Kaiser, M. Görner, C. C. Hilgetag, Criticality of spreading dynamics in hierarchical cluster networks without inhibition, *New J. Phys.* 9 (2007) 110.
- [27] J. M. Beggs, D. Plenz, Neuronal avalanches in neocortical circuits, *J. Neurosci.* 23 (2003) 1116711177.
- [28] T. Vojta, Rare region effects at classical, quantum and nonequilibrium phase transitions, *J. Phys. A* 39 (2006) R143.
- [29] M. A. Muñoz, R. Juhász, C. Castellano, G. Ódor, Griffiths phases on complex networks, *Phys. Rev. Lett.* 105 (12) (2010) 128701.
- [30] R. Juhász, G. Ódor, C. Castellano, M. A. Muñoz, Rare-region effects in the contact process on networks, *Phys. Rev. E* 85 (2012) 066125.

- [31] P. Villa Martín, P. Moretti, M. A. Muñoz, Rounding of abrupt phase transitions in brain networks, *J. Stat. Mech.* (2015) P01003.
- [32] P. Villegas, P. Moretti, M. A. Muñoz, Frustrated hierarchical synchronization and emergent complexity in the human connectome network, *Sci. Rep.* 4 (2014) 5990.
- [33] L. K. Gallos, H. A. Makse, M. Sigman, A small world of weak ties provides optimal global integration of self-similar modules in functional brain networks, *Proc. Natl. Acad. Sci. USA* 109 (2012) 2825–30.
- [34] S.-J. Wang, C. C. Hilgetag, C. Zhou, Sustained activity in hierarchical modular neural networks: Self-organized criticality and oscillations, *Front. Comput. Neurosci.* 5 (2011) 30.
- [35] F. R. K. Chung, *Spectral graph theory*, CBMS Regional Conference Series in Mathematics 92 (1997) 212.
- [36] M.-T. Hütt, M. Kaiser, C. C. Hilgetag, Perspective: network-guided pattern formation of neural dynamics, *Philosophical Transactions of the Royal Society B: Biological Sciences* 369 (1653) (2014) 20130522. doi: 10.1098/rstb.2013.0522.
- [37] F. Damicelli, C. C. Hilgetag, M.-T. Htt, A. Mess, Topological reinforcement as a principle of modularity emergence in brain networks, *Network Neuroscience* 3 (2) (2019) 589–605. doi:10.1162/netn_a_00085.
- [38] P. B. Graben, A. Jimenez-Marin, I. Diez, J. Cortes, M. Desroches, S. Rodrigues, Metastable resting state brain dynamics, *Front Comput Neurosci* 13 (2019) 62.
- [39] P. Cook, Y. Bai, S. Nadjati-Gilani, K. Seunarine, M. Hall, G. Parker, D. Alexander, Camino: Open-Source Diffusion-MRI Reconstruction and Processing, 14th Scientific Meeting of the International Society for Magnetic Resonance in Medicine (2006) 2759.

- [40] A. V. Goltsev, S. N. Dorogovtsev, J. G. Oliveira, J. F. F. Mendes, Localization and spreading of diseases in complex networks, *Phys. Rev. Lett.* 109 (2012) 128702.
- [41] M. Boguñá, C. Castellano, R. Pastor-Satorras, Nature of the epidemic threshold for the susceptible-infected-susceptible dynamics in networks, *Phys. Rev. Lett.* 111 (2013) 068701.
- [42] Z.-W. Wei, H. Liao, H.-F. Zhang, J.-R. Xie, W. B.-H., G.-L. Chen, Localized-endemic state transition in the susceptible-infected-susceptible model on networks, *arXiv:1704.02925*.
- [43] R. Mastrandrea, A. Gabrielli, F. Piras, G. Spalletta, G. Caldarelli, T. Gili, Organization and hierarchy of the human functional brain network lead to a chain-like core, *Scientific reports* 7 (1) (2017) 1–13.

Appendix

Imaging acquisition parameters

Same subject structure-function triple acquisitions were performed using a 3T Siemens Connectome Skyra with a 100 mT/m and 32-channel receive coils. The acquisition consisted of¹:

High-resolution anatomical MRI was acquired using a T1-weighted 3D MPRAGE sequence with the following parameters: TR=2400ms; TE=2.14ms; Flip angle=8deg; FOV=224×224 mm²; Voxel size=0.7mm isotropic; Acquisition time = 7 min and 40 sec.

Functional data at rest were acquired to obtain the blood-oxygenation-level-dependent (BOLD) signals with a gradient-echo EPI sequence with the following parameters: TR = 720ms, TE = 33.1ms; Flip angle = 52 deg; FOV = 208 ×

¹Here, we only report the parameters which are needed for the image preprocessing, but a complete information about the acquisitions can be found at <http://protocols.humanconnectome.org/HCP/3T/imaging-protocols.html>

180 mm²; Matrix = 104 × 90; 72 slices per volume, a total number of 1200 volumes; Voxel size = 2mm isotropic; Acquisition time = 14 min and 33 sec.

Diffusion data were acquired with a Spin-echo EPI sequence with the following parameters: TR = 5520ms; TE = 89.5ms; Flip angle = 78 deg; FOV = 210 × 180 mm²; Matrix = 168 × 144; 111 slices per volume; Voxel size = 1.25mm isotropic; 90 diffusion weighting directions plus 6 b=0 acquisitions; Three shells of b=1000, 2000, and 3000 s/mm²; Acquisition time: 9 min 50 sec.

Abbreviations

FC: functional connectivity HMN: hierarchical modular network MRI: magnetic resonance imaging SC: structural connectivity SIS: susceptible-infected-susceptible

Competing interests

The authors declare that they have no competing interests.

Ethics approval and consent to participate

The sample included 30 subjects from the MGH-USC Human Connectome Project. The research was performed in compliance with the Code of Ethics of the World Medical Association (Declaration of Helsinki). All subjects provided written informed consent, approved by the ethics committee in accordance with guidelines of HCP WU-Minn.

Funding

We acknowledge the Spanish Ministry and Agencia Estatal de investigación (AEI) through grant FIS2017-84256-P (European Regional Development Fund), as well as the Consejería de Conocimiento, Investigación y Universidad, Junta de Andalucía and European Regional Development Fund (ERDF), ref. SOMM17/6105/UGR for financial support. AS and PM acknowledge financial support from the Deutsche Forschungsgemeinschaft, under grants MO 3049/1-1 and MO 3049/3-1.

Availability of data and materials

Numerical simulation data are available on request from the corresponding author.

Author contributions

AS: Performed the simulations, Analyzed the data, Wrote the manuscript; PM: Designed the study, Analyzed the data, Wrote the manuscript; ID: Data curation, Preprocessed the images; JMC: Data curation, Wrote the manuscript. MAM: Designed the study, Analyzed the data, Wrote the manuscript

Acknowledgments